Published in final edited form as:

Phys Biol. ; 15(3): 031001. doi:10.1088/1478-3975/aa9e5e.

Mechanistic insights of the Min oscillator via cell-free reconstitution and imaging

Kiyoshi Mizuuchi[1] and **Anthony G. Vecchiarelli**[2,*]

[1]Laboratory of Molecular Biology, National Institute of Diabetes, and Digestive and Kidney Diseases, National Institutes of Health, Bethesda, MD 20892, USA

[2]Department of Molecular, Cellular and Developmental Biology, University of Michigan, Ann Arbor, MI 48109, USA

Abstract

The MinD and MinE proteins of *Escherichia coli* self-organize into a standing-wave oscillator on the membrane to help align division at mid-cell. When unleashed from cellular confines, MinD and MinE form a spectrum of patterns on artificial bilayers - static amoebas, traveling waves, traveling mushrooms, and bursts with standing-wave dynamics. We recently focused our cell-free studies on bursts because their dynamics recapitulate many features of Min oscillation observed *in vivo*. The data unveiled a patterning mechanism largely governed by MinE regulation of MinD interaction with membrane. We proposed that the MinD to MinE ratio on the membrane acts as a toggle switch between MinE-stimulated recruitment and release of MinD from the membrane. In this review, we summarize cell-free data on the Min system and expand upon a molecular mechanism that provides a biochemical explanation as to how these two 'simple' proteins can form the remarkable spectrum of patterns.

INTRODUCTION

The MinCDE system of *Escherichia coli* forms a cell-pole to cell-pole standing wave oscillator that prevents cell division near the cell poles[3–5]. MinD is an ATPase that, when bound to ATP, can dimerize and bind membrane via its membrane targeting sequence (MTS)[6–9]. MinE, the master controller of MinD-membrane interaction, also functions as a dimer with MTSs[10]. MinE-stimulated ATP hydrolysis by MinD is believed to be coupled to MinD release from the membrane[12]. The third and final component, MinC, is the inhibitor of divisome assembly[3,13,14]. MinC is a passenger protein on MinD that links MinD distribution on the membrane to divisome positioning. But MinC itself is not required for MinD/E oscillation[15,16]. The perpetual chase and release of MinD by MinE on the membrane produces a time-averaged concentration of MinC that is lowest at mid-cell[3,16–19]. The oscillation therefore promotes cell division at mid-cell by inhibiting division near the

*For Correspondence: Anthony G. Vecchiarelli, ave@umich.edu, Tel. 301-787-4292.

AUTHOR CONTRIBUTIONS

A.G.V. and K.M. wrote the paper. No authors have competing financial interests.

poles[4]. The remarkable oscillatory dynamics were first reported nearly 20 years ago[3,5,16], but the molecular mechanism remains unclear.

The Schwille and Mizuuchi groups, and very recently the Dekker group, have reconstituted Min patterning dynamics on supported lipid bilayers (SLBs) of varying lipid compositions[2,20–23] and under different confinement geometries[23–29]. Travelling waves of MinD chased by MinE was the first type of pattern to be reconstituted and analyzed on the bottom of an SLB-coated well[21]. In our SLB-coated flowcell, the Min system forms a variety of patterns[2]. Under constant flow, a near spatially homogeneous oscillation is generated, where large swaths of the SLB are bound and released by MinD and MinE[20,22]. Stopping the flow results in a pattern spectrum, where the MinD and MinE density on the SLB determines the mode of patterning – amoebas, waves, mushrooms or bursts (Fig. 1)[2]. At very high protein densities, MinD and MinE form amoebas - circular MinD binding zones of uniform size that are stably surrounded by an E-ring[20,22]. At moderate densities, MinD and MinE self-organize into travelling waves also observed by the Schwille and Dekker groups [21,23–29]. The protein densities within amoebas or waves are far in excess of what is possible *in vivo*. Also, these patterns lack standing-wave dynamics with nodes where the time-averaged local MinD concentration is minimum, as observed at mid-cell *in vivo*. Thus, it was difficult to decipher the mechanistic principles underlying these dissimilar patterns and how they relate to standing-wave oscillations *in vivo*.

We recently used our flowcell setup to specifically address the mechanistic basis for standing-wave oscillations. We hypothesized that to reconstitute a standing-wave in our flow cell, the MinD supply must be limiting because when a MinD polar zone develops *in vivo* the cytoplasmic pool of MinD presumably depletes[19]. Indeed under protein depletion conditions, we observed two previously unidentified patterns we called mushrooms and bursts (Fig. 1). Out of all patterns reconstituted on a flat SLB to date, our recent study focused on bursts as they were the only pattern to recapitulate the standing-wave dynamics observed *in vivo*. Recently, both the Dekker and Schwille groups have reconstituted similar standing wave dyanmics in microchambers with shapes and volumes similar to that of a bacterial cell [23,24,29]. The findings allowed us to propose a comprehensive molecular mechanism for standing-wave oscillations, which we explain in greater detail here [2].

Several recent reviews from the Schwille group highlight the remarkable progress in building cell division systems from the bottom-up using the purified MinCDE system and divisome components in microcompartments [30,31]. In this review, we summarize the cell-free data supporting a molecular mechanism that explains the variety of patterns supported by MinD and MinE both in and out of the cell; with an emphasis on the recent appreciation for how multiple conformational states of MinE can drive oscillation by spatiotemporally regulating MinD interaction with the membrane [2,10,32]. We first describe all known MinE conformations and our model. We then explain how the model relates to each pattern type. Finally we recap the mechanism from a temporal perspective - from pattern initiation to disassembly.

The Conformational Gymnastics of MinE

Our molecular mechanism of Min oscillation is inspired by the structures of MinD and MinE. MinE functions as a dimer with MTSs that were once considered to be largely 'inactive' while MinE is in solution[1,11,33]. This proposal arose from the fact that the MTSs in this latent state are packed against a six-stranded β-sheet at the dimer interface of MinE, stabilizing its hydrophobic core (Fig. 2A). But recent hydrogen-deuterium exchange and NMR experiments by the Lutkenhaus and Goto groups, respectively, as well as our unpublished MinE-SLB interaction studies have shown that the MTSs of the latent form of MinE are dynamically tethered to the six-stranded β-sheet, and can therefore reversibly interact with the membrane [10,32]. Adjacent to the MTSs are the MinD-binding domains that are buried in the hydrophobic core of the MinE dimer, unable to form the MinD-interacting interface. These cryptic MinD-binding domains are comprised of the inner-most-pair of β-strands at the dimer interface as well as coils connecting these β-strands to the MTSs. Thus, in solution, the MinD interaction interface of a MinE dimer is largely sequestered [1,11,33]. Upon interaction with MinD, this previously obstructed domain transitions to an α-helix (Fig. 2B–C)[10]. When MinE refolds into this 'active' state with a four-stranded β-sheet at the dimer interface, the membrane- and MinD-interaction domains readily bind their partners (Fig. 2C). Active MinE can associate with membrane-bound MinD, stabilize MinD on the membrane, and then stimulate MinD ATPase activity, which is thought to be coupled to MinD release from the membrane[2,12,34]. The molecular mechanism we describe in the next section provides a biochemical explaination as to how a MinE dimer can have multiple and seemingly counteracting roles in regulating MinD associations with membrane that ultimately drives oscillation.

The Model

Before any type of pattern is formed on the membrane, we propose that ATP-bound MinD dimers and MinE dimers of varying conformational states can transiently interact with the membrane (Fig. 3A). Local fluctuations in the MinD to MinE ratio on the membrane are needed to nucleate the formation of a radially expanding binding zone containing both MinD dimers alone (D_2) and those in complex with, and stabilized by, a MinE dimer (D_2E_2) (Fig. 3B). D_2E_2 not only stabilizes a MinD dimer on the membrane, but also acts to rapidly recruit more MinD dimers from solution *in vitro*, or from the cytoplasm *in vivo* (Fig. 3C). This is because the MinE dimer in the D_2E_2 complex has two MinD-interacting domains, but only one is occupied. The other could capture another MinD dimer. A corollary to this proposition is that a structural reason must exist to explain why the accessible MinD-interacting domain does not readily interact with a MinD dimer from another D_2E_2 complex. In other words, we suspect that the $D_2E_2D_2$complex has a key anti-cooperativity requirement in the patterning mechanism so as to prevent any higher order species, such as a MinD/MinE copolymer, but this remains to be further studied.

Upon nucleation of a patterning event, MinD rapidly binds the membrane starting at a nucleation site, where MinE also accumulates but more slowly. We propose that the slower binding rate of MinE stems from the dramatic structural transitions to its active form before it can stably bind membrane and MinD. Since there is more MinD than MinE present on the membrane during the initiation of a pattern, the majority of MinE dimers are in the D_2E_2 or

$D_2E_2D_2$ complex. A significant fraction of MinD dimers, free of MinE, could also accumulate on the membrane (Fig. 3D). But as the net MinD binding rate slows down, for reasons such as surface exclusion or solution depletion, MinE binding will eventually catch up and tip the balance. At this critical point, we propose another MinE dimer can now join a D_2E_2 complex to form $E_2D_2E_2$ – the MinD dissociation complex (Fig. 3E). This complex triggers the critical ATP hydrolysis by MinD required for its dissociation from membrane *via* an irreversible step. Since the formation of $E_2D_2E_2$ is coupled to the catalytic disassembly of the complex, we speculate that this intermediate would be difficult to directly observe. To summarize our model, the membrane-bound stoichiometry of MinD and MinE acts as the 'switch' from MinE-stimulated recruitment and stabilization of MinD on the membrane to MinE-stimulated release of MinD [2].

When a MinD dimer dissociates from the membrane, via the $E_2D_2E_2$ complex, the two MinE dimers responsible for its release can linger on the membrane (Fig. 3F). This lingering MinE species remains active for several seconds before reverting to its inactive form. During this time, it can associate with remaining D_2E_2 complexes on the surrounding membrane; releasing more MinD dimers while generating more lingering MinE dimers, forming a feedback loop. This catalytic release of MinD and self-amplification of lingering MinE would continue until essentially all local D_2E_2 complexes are depleted and is potentially involved in the formation of an E-ring. At this high density of lingering MinE, any MinD dimers binding from solution, or from neighboring areas of the membrane, would be quickly joined and disassembled by not one but two active MinE dimers (Fig. 3E–F). Lingering MinE therefore prevents MinD from rebinding regions of the membrane that other MinD dimers have just dissociated from, by quickly triggering ATP hydrolysis. In this model, stimulation of MinD membrane binding by MinE at the initial phase of pattern formation is an important preamble to the downstream triggering of ATP hydrolysis that disassembles the MinD dimer upon binding another MinE dimer. These requisite series of events are consistent with the finding that MinD binding to membrane is a prerequisite to MinE stimulation of ATP hydrolysis by MinD[2].

From an *in vivo* perspective, the mechanism would progress as follows. A significant density of lingering MinE provides the refractory period for MinD rebinding at the cell-pole from which it just dissociated (Fig. 4A). Once the lingering MinE density sufficiently declines, and the active MinD dimer concentration in the cytosol recovers, these MinE dimers are joined by MinD dimers in a one-to-one complex. This D_2E_2 complex stimulates the recruitment of more MinD to form $D_2E_2D_2$ complexes. The $D_2E_2D_2$ complex can readily release the MinD dimer to the surrounding membrane area after its recruitment, thereby continuing the positive feedback cycle (Fig. 4B–C). As active MinD dimers deplete from the cytosol and MinE accumulates on the membrane, $E_2D_2E_2$ then triggers the release of MinD and the lingering MinE dimers concentrate to form an E-ring (Fig. 4D). How MinE dimers concentrate to form a diffusion-resistant E-ring around the perimeter of a MinD polar zone [35,36] remains to be determined and is currently under study.

Standing-Wave Bursts

Bursts are radially expanding binding zones of MinD and MinE that initiate from random nucleation points on the SLB (Fig. 5; Movie 1). MinD binding during burst expansion is rapid whereas MinE slowly accumulates. As the local solution supply of the active MinD dimer depletes, burst expansion halts, its perimeter is corralled by an E-ring, and the burst implodes (Movie 1)[2]. We propose that during nucleation, a burst is composed of MinD dimers alone and in complex as D_2E_2 and $D_2E_2D_2$. When burst expansion slows down, MinE accumulates to a density that results in most MinD dimers associated with MinE in the one-to-one D_2E_2 complex. When the MinE density is high enough to form $E_2D_2E_2$ complexes, MinD is released from the membrane. This sequence results in a well-defined E-ring composed of lingering MinE around the burst perimeter, which is followed by burst implosion.

In our flowcell, a group of bursts collectively depleted active MinD dimers in the solution above a membrane area that was much larger than the size of an individual burst. Thus, a zone of bursts would initiate and disassemble in near synchrony. A subsequent group of bursts would form on other regions of the bilayer. The resulting subcycles oscillated with a temporal phase shift, which generated remarkable standing-wave dynamics[2]. We propose that the local density of lingering MinE remaining from a previous set of bursts provides the refractory period for MinD in solution from immediately binding that same region of the membrane. Once this lingering MinE density declines, it can once again stimulate MinD recruitment and burst nucleation in the form of D_2E_2 complexes.

The characteristic spatial dimension of the synchronous burst zones was ~25 μm. We believe this number reflects the diffusion-limited depletion of active MinD in solution[2] and the open geometry of the flowcell that has a very low membrane surface to solution volume ratio compared to a bacterial cell. Inside an *E. coli* cell that is much smaller than our flowcell, MinD depletion is not diffusion-limited and the small membrane area can only accommodate a single burst at a time (i.e. a MinD polar binding zone). Consistently, a standing-wave oscillation more closely resembling the *in vivo* dynamics has been observed *in vitro* by confining the reaction in microfluidic chambers coated with an SLB[23,24,28,29]. These observations support the notion that differences in reaction vessel geometry cause the difference in appearance between the standing-wave oscillation observed *in vivo* and the burst dynamics in our flowcell.

The above discussion is based on the premise that, at the onset of burst initiation in our flowcell or MinD polar binding zone *in vivo*, the distribution of active MinD dimers in solution/cytosol is essentially homogeneous. This certainly would be the case *in vivo* considering the time scale difference of MinD diffusion in the cytoplasm (< 1 sec) and the oscillation cycle (seconds). In our flow cell, during the ~10 sec period of burst growth, we believe the solution supply of active MinD is locally depleted. The total MinD concentration in solution decreased ~ 20% during this period[2], indicating that ~ 80% of MinD in solution was still inactive, waiting to become ready to bind the membrane. *In vivo* fluorescence correlation spectroscopy experiments also suggest that roughly two-thirds of total MinD molecules are inactive in the cytosol [37]. These observations are incompatible with the notion that reactivation of MinD after ATP hydrolysis and membrane dissociation takes place

rapidly. Thus, the MinD re-activation delay time, which remains to be directly measured, is expected to be long enough such that newly reactivated MinD emerges homogeneously throughout the reaction volume, guaranteeing a spatially homogeneous distribution of MinD ready to bind membrane at the onset of each burst cycle.

Travelling Mushrooms

Mushrooms were an intermediate pattern between travelling waves and bursts where the MinD supply was semi-depleted (Fig. 6; Movie 1)[2]. When a mushroom formed, its peak local MinD protein density reached 8000 ± 2000 dimers/μm^2, which equates to ~ 25% surface confluency. Like bursts, mushrooms temporally oscillated as expanding binding zones of MinD that were corralled and disassembled by MinE. In contrast to individual bursts, which were symmetric and spatially disconnected from one another, mushrooms budded out from the previous disassembling set of mushrooms, resulting in an asymmetric propagation of the MinD binding zone, which was followed by a spatially skewed disassembly by MinE. After the MinD binding front of a mushroom stalled and was corralled by an E-ring, the spatial asymmetry was propagated by subsequent mushrooms. As the density of MinD and MinE proteins increased on the SLB and with the higher MinD supply in solution, the MinD binding front was not stalled by an E-ring, and mushrooms merged to form continuous travelling waves.

Travelling Waves

Travelling waves are the most persistent and stable pattern formed *in vitro* on flat SLBs (Fig. 7A; Movie 1) [2,21,22,24,25,27,29,38]. At a wave front, both MinD and MinE bind the membrane; MinD binds quickly whereas MinE slowly accumulates. We propose the wave front is primarily composed of MinD dimers alone (D_2) and in D_2E_2 and $D_2E_2D_2$ complexes just like the expansion phase of a burst. Towards the rear of the wave after the MinD density plateaus, MinE accumulates to a density that results in the majority of MinD dimers sequestered in the one-to-one D_2E_2 complex. Here, the MinE density is now high enough to start forming $E_2D_2E_2$ complexes that triggers ATP hydrolysis and precipitously releases MinD from the membrane. This results in a well-defined band of lingering MinE dimers at the wave rear, similar to the E-ring around bursts. As described in our model, the significant density of MinE lingering behind a wave provides the refractory period for MinD rebinding the membrane. But once the density of lingering MinE declines, with ATP-MinD steadily arriving from solution, the MinD-to-MinE stoichiometry on the surface once again rises above one and MinE assists in accelerating MinD binding to the membrane as D_2E_2 complexes, which initiates the next wave front.

When increasing the MinE concentration in the reaction, while keeping MinD constant, we found a corresponding increase in the rate of MinD binding at the wave front, once again supporting our proposal that MinE stimulates MinD recruitment to membrane (Fig. 7B). However, the peak MinD density achieved within a wave is essentially the same − 8000 ± 2000 MinD dimers/μm^2, which equates to ~ 25% surface confluency. At this density, surface area exclusion effects become highly significant (see below). MinE also accumulates faster with higher MinE in solution; reaching the peak MinE density quicker and starting the disassembly phase earlier. As a result, more MinE in solution narrows the width of the MinD

band of a wave (Fig. 7C). Thus, once MinE-stimulated disassembly of MinD starts, it occurs at a similar rate. However, the wavelength remains constant presumably because it takes longer for the lingering MinE density to reach a low enough level for the subsequent wavefront progression. The findings are consistent with the proposal that membrane-associated MinE has counteracting influences on MinD-membrane association that depends on the phase within the pattern cycle, and the MinD/MinE ratio on the membrane.

Travelling waves versus standing-wave bursts

Using our molecular mechanism, we can explain how the Min system creates both waves and bursts on an SLB. As with wave initiation, increasing the MinE concentration results in an increased rate of MinD binding during burst initiation and expansion, and the periodicity remains constant (Fig. 7D). Unlike waves however, the peak MinD density within bursts decreases with less MinE in solution (Fig. 7E). Bursts were the only pattern supported by protein densities that do not reach the effective saturation point of ~8000 ± 2000 MinD dimers/μm^2 (~ 25% surface confluency). As MinD binding slows due to solution depletion, MinE binding catches up and disassembles the burst. In the solution phase above wave patterns on the SLB, the MinD and MinE protein distribution is effectively homogeneous [2,20–22], and the protein amounts are well in excess of that found *in vivo* [36]. We conclude that bursts undergoing a standing-wave oscillation switch to disassembly due to the local depletion of active MinD in solution. But for waves, solution depletion does not set the limit for MinD density on the SLB. Rather, we believe that protein-membrane associations become strongly inhibited by surface exclusion. Consistently, the peak MinD protein density in waves does not exceed ~25% of the surface density at confluence. At this density, the binding rate is expected to become very low due to surface area exclusion effects, deviating from predictions based on the Langmuir adsorption model[39,40]. As the surface densities of MinD dimers and D_2E_2 complexes become higher than ~ 10% confluence, the rate of MinD binding will slow faster than MinE because MinE has a smaller footprint on the SLB. Without necessarily involving ATP hydrolysis, both MinD dimers and D_2E_2 complexes can dissociate from the SLB with an apparent k_{off} of ~ 0.2 s^{-1} and ~ 0.03 s^{-1}, respectively[2]. By competition for membrane area, MinE would start displacing MinD already on the membrane. Once D_2E_2 complexes becomes the more prevalent complex on the SLB, $E_2D_2E_2$ would eventually form and start dissociating MinD dimers from the SLB; making even more room for MinE binding. This scenario conveniently explains the plateau and decline of MinD that is accompanied by a transient acceleration of MinE binding just before the MinD to MinE ratio switches[20]. To put it simply, MinD stops binding within a wave because there is no more room on the SLB, whereas in bursts (or in a MinD polar zone *in vivo*), MinD stops binding because the solution (or cytosolic) supply has depleted.

Amoebas

A major question remaining to be experimentally addressed is how does MinE coalesce into a dense, well-defined E-ring that resists diffusion (see Fig. 4D)? It has been proposed that MinE dimers self-assemble into higher-order oligomers to form an E-ring. A truncated MinE variant lacking its dimerization domain has been shown to form amyloids on an SLB *in vitro* [41,42]. But these mutants are not functional *in vivo*, and amyloids by their nature do not readily disassemble; a key requirement for oscillatory dynamics.

The amoeba mode of patterning may provide insight (Fig. 8). Like bursts, amoebas have a core composed of both MinD and MinE corralled by an E-ring. Unlike bursts, amoebas are relatively static and the E-ring is very stable. Also, under a given set of reaction conditions, amoebas are uniform in size. If an amoeba grew larger than this characteristic size, it divided in two or more. If it shrunk, the amoeba would implode. Therefore, although not as mobile as the other modes of patterning, amoebas are still in a state of protein flux as also confirmed by FRAP measurements [20].

What maintains this positional memory? We suggest these observations reflect a local transition in membrane structure and/or composition caused by MinE binding, which then acts as a positive feedback loop for further local stabilization of MinE on the membrane. Stable amoebas and MinE-mesh patterns reported earlier[20] could be exacerbated manifestations of MinE's ability to condense into a thin tight E-ring without significant diffusional spreading by inducing local changes in membrane state [2]. It is possible that MinE binding to membrane *in vivo* promotes dynamic local membrane inhomogeneities that stabilize the E-ring (see Fig. 4D). The nature of these membrane inhomogeneities remains to be further investigated and could shed light on how MinE dimers cooperatively form an E-ring without polymerizing into a filament. Future studies will further probe whether MinE binding can cause membrane transitions that promote E-ring condensation.

MinE may dynamically associate with membrane independent of MinD

Our discussion thus far has focused on what MinD and MinE are doing within a pattern. But what is happening on the membrane prior to pattern organization? In our cell-free experiments, the 'background' MinE density on the SLB prior to pattern formation was not zero [2,20,22]. Also, in buffers of lower ionic strength, or if the bilayer has a high content of anionic lipid, membrane binding by MinE has been shown to be significant, even without MinD[22,34,41,43]. From this, our model proposes that inactive MinE dimers in solution are in equilibrium with a proportion that can interact with membrane.

It is attractive to speculate that the MTSs of a closed MinE dimer can transiently flip out and interact with membrane, but then quickly revert back to the inactive state (see Fig. 3A, middle). Without MinD present, active MinE dimers are therefore not expected to significantly accumulate on the membrane (see Fig. 3A, right). However, if one of these brief membrane associations allow MinE to encounter a membrane-bound MinD dimer, the interaction could promote refolding of MinE and unveil the entire MinD interacting α-helix (see Fig. 3B). The resulting D_2E_2 complex would stabilize both MinD and MinE dimers on the membrane with a total of three interacting MTSs - two from the MinD dimer and one from the MinE dimer. Incorporation of a MinE dimer into the D_2E_2 complex is slow because of the major structural transition in MinE required to go from a six- to four-stranded β-sheet at the dimer interface. Therefore, we propose that the 'inactive' state of MinE in solution acts as a buffer for the active membrane-bound MinE populations. Our proposal of MinE membrane binding prior to the nucleation of a pattern is based on experiments in the presence of MinD and therefore do not necessarily reflect MinD-independent membrane binding [2]. A direct measure of the equilibrium density of MinE dimers in the absence of MinD on an SLB is a focus of current research.

Patterns initiate by MinE locally stimulating MinD binding to the membrane

Nonlinear kinetics are essential for many self-organizing processes. Positive feedback loops can fulfill this requirement. Many previous models postulate that pole-to-pole oscillations result from MinD first binding the cell-pole *via* an enigmatic auto-catalytic process as first postulated by Meinhardt and DeBoer[19], and followed by many others[44–50]. Reconstituting such a process *in vitro* would predict sigmoidal binding kinetics with an exponential phase, and in the clearest cases, MinD binding would initiate stochastically from isolated nucleation points on the SLB. We consistently found that MinD on its own steadily and uniformly bound the SLB without any sign of auto-catalytic binding from a nucleation center, or sigmoidal rate acceleration after the initial binding event[20]. We conclude that when MinD dimers bind membrane without MinE, there is no notable positive feedback loop operating to form auto-catalytic MinD binding centers.

In stark contrast, when MinE is present, a short period of low-level uniform binding by MinD and MinE is followed by local explosive MinD binding from nucleation points on the SLB - a clear catalytic initiation of MinD membrane binding in the presence of MinE[2,20,22]. The cell-free data strongly suggest that MinE plays a critical role in the MinD binding positive feedback loop that is required for the rapid radial expansion of a MinD polar zone *in vivo*.

Previous bulk biochemical studies have shown that MinD binding to membrane is cooperative[51–53]. As MinD binds membrane in its dimeric form, cooperative membrane binding with a Hill coefficient up to two[51] is to be expected in these steady state binding studies. This type of “cooperativity” is likely a simple reflection of the law of mass action operating in steady state, and should not be confused as an indicator of a non-linear kinetic process such as autocatalysis, or a positive feedback loop.

Lingering MinE inhibits MinD binding and provides the refractory period for oscillation

According to our model, D_2E_2 can either (*i*) bind another lingering MinE dimer, form $E_2D_2E_2$, and dissociate the MinD dimer from membrane *via* ATP hydrolysis, or (*ii*) recruit another MinD dimer to the membrane from solution faster than MinD binding on its own. When the lingering MinE density is high, MinD dimers trying to bind from solution will encounter two lingering MinE dimers in quick succession and get recycled back into solution. Prevention of MinD binding by lingering MinE dimers sets the refractory period for oscillation. During this period, the lingering MinE density slowly declines. But instead of completely disappearing, it diminishes towards a low level.

While the lingering MinE density is declining, the concentration of active MinD dimers in solution is recovering. Then, at a critical point, the probability becomes significant enough for MinE-stimulated nucleation of MinD membrane binding to take over. We expect the ratio of MinD to MinE on the membrane would again be approaching one at this point, with MinD and MinE dimers residing on the membrane mainly as D_2E_2 complexes. At this low level of protein species on the membrane, local fluctuations leads to stochastic nucleation of individual binding zones on the SLB[2,20,22]. After successful nucleation, the expanding

MinD/MinE binding zone forms a binding propagation front at the outer edge, which supersedes the *de novo* nucleation of additional binding events.

Lingering MinE is not restricted to 2D diffusion on the membrane. Rather, it can also diffuse briefly in solution. This active form of MinE in solution likely reverts back to the inactive state well within a second or rebinds membrane, thus limiting its bulk diffusion distance. Solution diffusion of this MinE species explains our previous observation of circular MinD binding zones breaking symmetry to form waves that only travel upstream during sample flow[22]. Sample flow pushes the diffusible lingering MinE species downstream, thus only permitting upstream MinD binding and wave propagation. In the absence of flow, it is likely that lingering MinE can diffuse in solution above the SLB and have a significant radius of action to influence local Min patterning. When a propagating wave approaches an amoeba for example, the wave seems to sense the E-ring of the amoeba at a distance, which then deforms the wave front[20]. Spatial communication among patterns by this diffusible state of lingering MinE can also explain the previously reported wave phase synchronization across membrane gaps[25].

CONCLUSIONS

A large body of cell-free observations has allowed us to propose the first comprehensive molecular mechanism that attempts to explain the wide variety of patterns achievable by MinD and MinE self-organization on a membrane[2]. Although only two proteins are required for patterning, this ‘simple’ system actually involves a large number of key molecular species. Contrary to previous models showing MinD binding to the membrane in an autocatalytic process and MinE coming along only to kick it off, the careful analysis of a wide variety of patterns observed *in vitro* strongly suggest that MinE orchestrates the entire oscillatory process through regulation of MinD membrane binding. Cell-free studies will continue to test the model described here whereby MinE successively recruits, stabilizes, releases and inhibits MinD interactions with membrane to drive oscillation. However, *in vitro* study alone can only go so far. A systematic study of Min oscillation *in vivo* must be continued to test many of the assumptions made in our model. For example, MinC shares the same interface as MinE for binding MinD, therefore our mechanism has implications for MinC dynamics on the inner membrane, which will be a focus of future study.

Since 2001, there have been numerous attempts to mathematically model and simulate the Min system[19,44–50,54–62]. Previous mathematical modeling exercises were based on the limited experimental data available, and by necessity, the number of significant molecular species considered had to be kept to a minimum. Each of these modeling attempts are founded on the basis of different molecular mechanisms, yet they all can reproduce certain aspects of Min dynamics. These exercises show that there are many ways to generate an oscillator *in silico*. But as biologists, our goal is to elucidate the oscillatory mechanism developed by evolution. No previous model we are aware of has globally reproduced the spectrum of patterns supported by the Min system both *in vivo* and *in vitro*. Our recent work suggests previous models are not only oversimplifications, they have missed a number of reaction elements that are critical for the architecture of the mechanism. On the other hand, many of the molecular complexes proposed here still remain hypothetical and only a small

subset of reaction parameters have been estimated directly to assist computational simulation. A systematic biochemical study and quantitative analysis of each reaction step is essential to confirm many aspects of our proposed mechanism as well as to impose constraints on the rate parameters involved. These experimental approaches, combined with quantitative simulations, will further refine and improve our understanding of this fascinating and beautiful system.

Supplementary Material

Refer to Web version on PubMed Central for supplementary material.

Acknowledgments

This work was supported by the intramural research fund for NIDDK (to K.M.), NIH US Dept of HHS, and the Nancy Nossal Fellowship (to A.G.V.).

References

1. Ghasriani H, et al. Appropriation of the MinD protein-interaction motif by the dimeric interface of the bacterial cell division regulator MinE. Proc Natl Acad Sci USA. 2010; 107:18416–18421. DOI: 10.1073/pnas.1007141107 [PubMed: 20937912]
2. Vecchiarelli AG, et al. Membrane-bound MinDE complex acts as a toggle switch that drives Min oscillation coupled to cytoplasmic depletion of MinD. Proc Natl Acad Sci USA. 2016; 113:E1479–E1488. DOI: 10.1073/pnas.1600644113 [PubMed: 26884160]
3. Hu Z, Lutkenhaus J. Topological regulation of cell division in Escherichia coli involves rapid pole to pole oscillation of the division inhibitor MinC under the control of MinD and MinE. Mol Microbiol. 1999; 34:82–90. DOI: 10.1046/j.1365-2958.1999.01575.x [PubMed: 10540287]
4. Lutkenhaus J. Assembly Dynamics of the Bacterial MinCDE System and Spatial Regulation of the Z Ring. Annu Rev Biochem. 2007; 76:539–562. DOI: 10.1146/annurev.biochem.75.103004.142652 [PubMed: 17328675]
5. Raskin DM, de Boer PAJ. Rapid pole-to-pole oscillation of a protein required for directing division to the middle of *Escherichia coli*. Proc Natl Acad Sci USA. 1999a; 96:4971–4976. [PubMed: 10220403]
6. Hu ZL, Lutkenhaus J. A conserved sequence at the C-terminus of MinD is required for binding to the membrane and targeting MinC to the septum. Mol Microbiol. 2003; 47:345–355. [PubMed: 12519187]
7. Szeto TH, Rowland SL, Rothfield LI, King GF. Membrane localization of MinD is mediated by a C-terminal motif that is conserved across eubacteria, archaea, and chloroplasts. Proc Natl Acad Sci USA. 2002; 99:15693–15698. DOI: 10.1073/pnas.232590599 [PubMed: 12424340]
8. Wu W, Park KT, Holyoak T, Lutkenhaus J. Determination of the structure of the MinD–ATP complex reveals the orientation of MinD on the membrane and the relative location of the binding sites for MinE and MinC. Mol Microbiol. 2011; 79:1515–1528. [PubMed: 21231967]
9. Zhou H, Lutkenhaus J. Membrane Binding by MinD Involves Insertion of Hydrophobic Residues within the C-Terminal Amphipathic Helix into the Bilayer. J Bacteriol. 2003; 185:4326–4335. DOI: 10.1128/jb.185.15.4326-4335.2003 [PubMed: 12867440]
10. Park K-T, Villar MT, Artigues A, Lutkenhaus J. MinE conformational dynamics regulate membrane binding, MinD interaction, and Min oscillation. Proc Natl Acad Sci USA. 2017; 114:7497–7504. DOI: 10.1073/pnas.1707385114 [PubMed: 28652337]
11. Park KT, et al. The Min Oscillator Uses MinD-Dependent Conformational Changes in MinE to Spatially Regulate Cytokinesis. Cell. 2011; 146:396–407. [PubMed: 21816275]
12. Hu Z, Gogol EP, Lutkenhaus J. Dynamic assembly of MinD on phospholipid vesicles regulated by ATP and MinE. Proc Natl Acad Sci USA. 2002; 99:6761–6766. DOI: 10.1073/pnas.102059099 [PubMed: 11983867]

13. Cordell SC, Lowe J. Crystal Structure of the bacterial cell division regulator MinD. FEBS Lett. 2001; 492:160–165. [PubMed: 11248256]
14. Dajkovic A, Lan G, Sun SX, Wirtz D, Lutkenhaus J. MinC Spatially Controls Bacterial Cytokinesis by Antagonizing the Scaffolding Function of FtsZ. Curr Biol. 2008; 18:235–244. doi:http://dx.doi.org/10.1016/j.cub.2008.01.042. [PubMed: 18291654]
15. Hu Z, Lutkenhaus J. Analysis of MinC Reveals Two Independent Domains Involved in Interaction with MinD and FtsZ. J Bacteriol. 2000; 182:3965–3971. DOI: 10.1128/jb.182.14.3965-3971.2000 [PubMed: 10869074]
16. Raskin DM, de Boer PAJ. MinDE-Dependent Pole-to-Pole Oscillation of Division Inhibitor MinC in Escherichia coli. J Bacteriol. 1999b; 181:6419–6424. [PubMed: 10515933]
17. Fu X, Shih YL, Zhang Y, Rothfield LI. The MinE ring required for proper placement of the division site is a mobile structure that changes its cellular location during the Escherichia coli division cycle. Proc Natl Acad Sci USA. 2001; 98:980–985. [PubMed: 11158581]
18. Hale CA, Meinhardt H, de Boer PAJ. Dynamic localization cycle of the cell division regulator MinE in Escherichia coli. EMBO J. 2001; 20:1563–1572. DOI: 10.1093/emboj/20.7.1563 [PubMed: 11285221]
19. Meinhardt H, de Boer PAJ. Pattern formation in Escherichia coli: A model for the pole-to-pole oscillations of Min proteins and the localization of the division site. Proc Natl Acad Sci USA. 2001; 98:14202–14207. DOI: 10.1073/pnas.251216598 [PubMed: 11734639]
20. Ivanov V, Mizuuchi K. Multiple modes of interconverting dynamic pattern formation by bacterial cell division proteins. Proc Natl Acad Sci USA. 2010; 107:8071–8078. DOI: 10.1073/pnas.0911036107 [PubMed: 20212106]
21. Loose M, Fischer-Friedrich E, Ries J, Kruse K, Schwille P. Spatial Regulators for Bacterial Cell Division Self-Organize into Surface Waves *in vitro*. Science. 2008; 320:789–792. DOI: 10.1126/science.1154413 [PubMed: 18467587]
22. Vecchiarelli AG, Li M, Mizuuchi M, Mizuuchi K. Differential affinities of MinD and MinE to anionic phospholipid influence Min patterning dynamics in vitro. Mol Microbiol. 2014; 93:453–463. DOI: 10.1111/mmi.12669 [PubMed: 24930948]
23. Zieske K, Schwille P. Reconstitution of self-organizing protein gradients as spatial cues in cell–free systems. eLife. 2014; 3
24. Caspi Y, Dekker C. Mapping out Min protein patterns in fully confined fluidic chambers. eLife. 2016; 5:e19271. [PubMed: 27885986]
25. Schweizer J, et al. Geometry sensing by self-organized protein patterns. Proc Natl Acad Sci USA. 2012; 109:15283–15288. DOI: 10.1073/pnas.1206953109 [PubMed: 22949703]
26. Zieske K, Chwastek G, Schwille P. Protein Patterns and Oscillations on Lipid Monolayers and in Microdroplets. Angew Chem Int Ed Engl. 2016; 55:13455–13459. DOI: 10.1002/anie.201606069 [PubMed: 27465495]
27. Zieske K, Schweizer J, Schwille P. Surface topology assisted alignment of Min protein waves. FEBS Letters. 2014; 588:2545–2549. DOI: 10.1016/j.febslet.2014.06.026 [PubMed: 24937143]
28. Zieske K, Schwille P. Reconstitution of Pole-to-Pole Oscillations of Min Proteins in Microengineered Polydimethylsiloxane Compartments. Angew Chem Int Ed Engl. 2013; 52:459–462. DOI: 10.1002/anie.201207078 [PubMed: 23184489]
29. Kretschmer S, Zieske K, Schwille P. Large-scale modulation of reconstituted Min protein patterns and gradients by defined mutations in MinE's membrane targeting sequence. PLOS ONE. 2017; 12:e0179582. [PubMed: 28622374]
30. Kretschmer S, Schwille P. Pattern formation on membranes and its role in bacterial cell division. Curr Opin Cell Biol. 2016; 38:52–59. doi:http://dx.doi.org/10.1016/j.ceb.2016.02.005. [PubMed: 26915065]
31. Loose, M., Zieske, K., Schwille, P. Prokaryotic Cytoskeletons: Filamentous Protein Polymers Active in the Cytoplasm of Bacterial and Archaeal Cells. Löwe, Jan, Amos, Linda A., editors. Springer International Publishing; 2017. p. 419-444.
32. Ayed SH, et al. Dissecting the role of conformational change and membrane binding by the bacterial cell division regulator MinE in the stimulation of MinD ATPase activity. J Biol Chem. 2017

33. Kang GB, et al. Crystal structure of Helicobacter pylori MinE, a cell division topological specificity factor. Mol Microbiol. 2010; 76:1222–1231. DOI: 10.1111/j.1365-2958.2010.07160.x [PubMed: 20398219]
34. Hsieh C-W, et al. Direct MinE–membrane interaction contributes to the proper localization of MinDE in E. coli. Mol Microbiol. 2010; 75:499–512. DOI: 10.1111/j.1365-2958.2009.07006.x [PubMed: 20025670]
35. Raskin DM, de Boer PAJ. The MinE Ring: An FtsZ-Independent Cell Structure Required for Selection of the Correct Division Site in *E. coli*. Cell. 1997; 91:685–694. [PubMed: 9393861]
36. Shih YL, Fu X, King GF, Le T, Rothfield L. Division site placement in E.coli: mutations that prevent formation of the MinE ring lead to loss of the normal midcell arrest of growth of polar MinD membrane domains. EMBO J. 2002; 21:3347–3357. DOI: 10.1093/emboj/cdf323 [PubMed: 12093736]
37. Meacci G, et al. Mobility of Min-proteins in Escherichia coli measured by fluorescence correlation spectroscopy. Phys Biol. 2006; 3:255. [PubMed: 17200601]
38. Loose M, Fischer-Friedrich E, Herold C, Kruse K, Schwille P. Min protein patterns emerge from rapid rebinding and membrane interaction of MinE. Nat Struct Mol Biol. 2011; 18:577–583. [PubMed: 21516096]
39. Schaaf P, Talbot J. Kinetics of Random Sequential Adsorption. Phys Rev Lett. 1989; 62:175–178. [PubMed: 10039942]
40. Talbot J, Jin X, Wang NHL. New Equations for Multicomponent Adsorption Kinetics. Langmuir. 1994; 10:1663–1666. DOI: 10.1021/la00018a009
41. Zheng M, et al. Self-Assembly of MinE on the Membrane Underlies Formation of the MinE Ring to Sustain Function of the Escherichia coli Min System. J Biol Chem. 2014; 289:21252–21266. DOI: 10.1074/jbc.M114.571976 [PubMed: 24914211]
42. Chiang Y-L, et al. Atomic Force Microscopy Characterization of Protein Fibrils Formed by the Amyloidogenic Region of the Bacterial Protein MinE on Mica and a Supported Lipid Bilayer. PLOS ONE. 2015; 10:e0142506. [PubMed: 26562523]
43. Shih Y-L, et al. The N-Terminal Amphipathic Helix of the Topological Specificity Factor MinE Is Associated with Shaping Membrane Curvature. PLoS ONE. 2011; 6:e21425. [PubMed: 21738659]
44. Arjunan SNV, Tomita M. A new multicompartmental reaction-diffusion modeling method links transient membrane attachment of E. coli MinE to E-ring formation. Syst Synth Biol. 2010; 4:35–53. DOI: 10.1007/s11693-009-9047-2 [PubMed: 20012222]
45. Hoffmann M, Schwarz US. Oscillations of Min-proteins in micropatterned environments: a three-dimensional particle-based stochastic simulation approach. Soft Matter. 2014; 10:2388–2396. DOI: 10.1039/C3SM52251B [PubMed: 24622920]
46. Bonny M, Fischer-Friedrich E, Loose M, Schwille P, Kruse K. Membrane Binding of MinE Allows for a Comprehensive Description of Min-Protein Pattern Formation. PLoS Comput Biol. 2013; 9:e1003347. [PubMed: 24339757]
47. Huang KC, Meir Y, Wingreen NS. Dynamic structures in Escherichia coli: Spontaneous formation of MinE rings and MinD polar zones. Proc Natl Acad Sci USA. 2003; 100:12724–12728. DOI: 10.1073/pnas.2135445100 [PubMed: 14569005]
48. Huang KC, Wingreen NS. Min-protein oscillations in round bacteria. Phys Biol. 2004; 1:229. [PubMed: 16204843]
49. Halatek J, Frey E. Highly Canalized MinD Transfer and MinE Sequestration Explain the Origin of Robust MinCDE-Protein Dynamics. Cell Rep. 2012; 1:741–752. doi:http://dx.doi.org/10.1016/j.celrep.2012.04.005. [PubMed: 22813748]
50. Fange D, Elf J. Noise-Induced Min Phenotypes in E. coli. PLOS Computational Biology. 2006; 2:e80. [PubMed: 16846247]
51. Mileykovskaya E, et al. Effects of Phospholipid Composition on MinD-Membrane Interactions *in vitro* and *in vivo*. J Biol Chem. 2003; 278:22193–22198. DOI: 10.1074/jbc.M302603200 [PubMed: 12676941]
52. Lackner LL, Raskin DM, de Boer PAJ. ATP-Dependent Interactions between *Escherichia coli* Min Proteins and the Phospholipid Membrane In Vitro. J Bacteriol. 2003; 185:735–749. DOI: 10.1128/jb.185.3.735-749.2003 [PubMed: 12533449]

53. Renner LD, Weibel DB. MinD and MinE Interact with Anionic Phospholipids and Regulate Division Plane Formation in Escherichia coli. J Biol Chem. 2012; 287:38835–38844. DOI: 10.1074/jbc.M112.407817 [PubMed: 23012351]

54. Meacci G, Kruse K. Min-oscillations in Escherichia coli induced by interactions of membrane-bound proteins. Phys Biol. 2005:89–97. DOI: 10.1088/1478-3975/2/2/002 [PubMed: 16204861]

55. Fischer-Friedrich E, Nguyen van yen R, Kruse K. Surface waves of Min-proteins. Phys Biol. 2007; 4:38. [PubMed: 17406084]

56. Thalmeier D, Halatek J, Frey E. Geometry-induced protein pattern formation. Proc Natl Acad Sci USA. 2016; 113:548–553. DOI: 10.1073/pnas.1515191113 [PubMed: 26739566]

57. Derr J, Hopper JT, Sain A, Rutenberg AD. Self-organization of the MinE protein ring in subcellular Min oscillations. Phys Rev E. 2009; 80:011922.

58. Sengupta S, Derr D, Sain A, Rutenberg AD. Stuttering Min oscillations within E. coli bacteria: a stochastic polymerization model. Phys Biol. 2012; 9:056003. [PubMed: 22931851]

59. Krstić V, Maglica Ž, Paljetak HČ, Podobnik B, Pavin N. Min-Protein Oscillations in E. coli: Three-Dimensional Off-Lattice Stochastic Reaction- Diffusion Model. J Stat Phys. 2007; 128:5–20. DOI: 10.1007/s10955-006-9189-5

60. Pavin N, Paljetak HČ, Krstić V. Min-protein oscillations in \textit{Escherichia coli} with spontaneous formation of two-stranded filaments in a three-dimensional stochastic reaction-diffusion model. Physical Review E. 2006; 73:021904.

61. Borowski P, Cytrynbaum EN. Predictions from a stochastic polymer model for the MinDE protein dynamics in Escherichia coli. Physical Review E. 2009; 80:041916.

62. Cytrynbaum EN, Marshall BDL. A Multistranded Polymer Model Explains MinDE Dynamics in E. coli Cell Division. Biophysical Journal. 2007; 93:1134–1150. doi:https://doi.org/10.1529/biophysj.106.097162. [PubMed: 17483175]

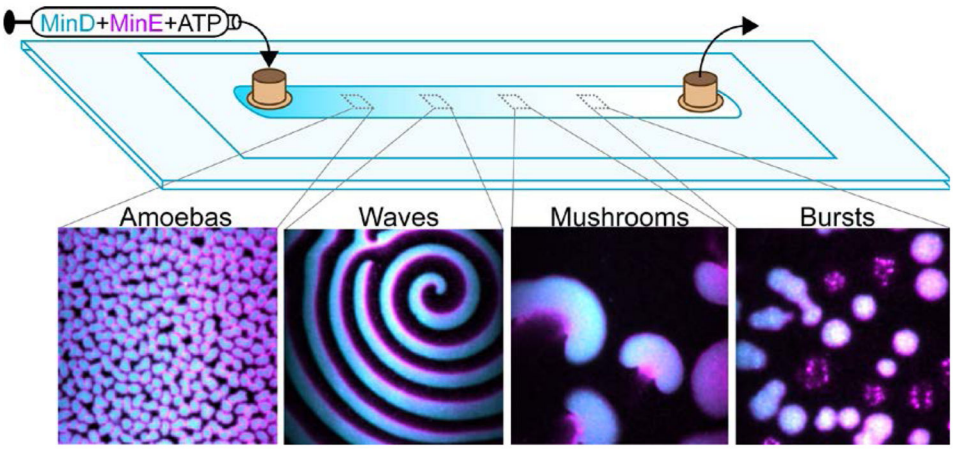

Fig. 1. MinD and MinE form a spectrum of cell-free patterns on a flat bilayer

(**A**) GFP-MinD (cyan) and MinE-Alexa647 (magenta) were pre-incubated with ATP and infused into a flowcell coated with a supported lipid bilayer (SLB). Observed patterns were recorded after sample flow was stopped. Still images were adapted from Vecchiarelli et al., 2016 showing the different modes of patterning supported by the decreasing GFP-MinD density on the SLB from inlet to outlet.

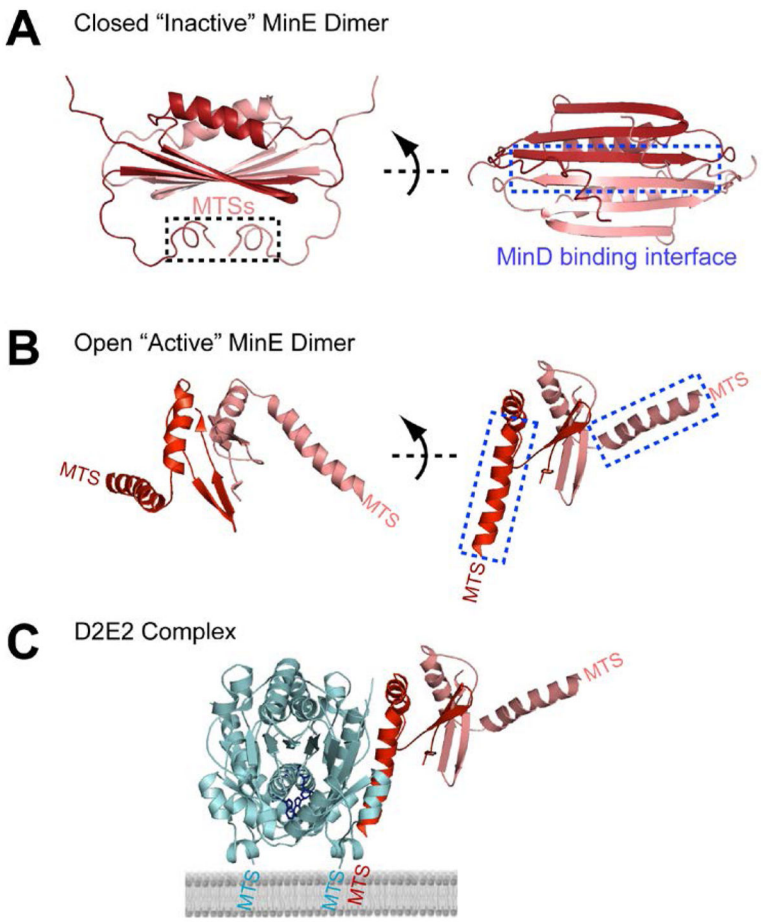

Fig. 2. The conformational gymnastics of MinE

(**A**) The ‘inactive’ or closed structure of the MinE dimer adapted from PDB ID 2KXO[1]. MinD binding domains comprise the dimer interface as well as the loops that connect to the adjacent Membrane Targeting Sequences (MTSs). The MTSs are tacked onto this hydrophobic core. In this closed form, the MinD interaction interface is occluded. (**B**) The ‘active’ or open structure of the MinE dimer in its MinD-interacting conformation. The once buried MinD binding interfaces and adjacent MTSs are now accessible for interaction. The MinD-interaction domains are likely in a random coil conformation when not bound to MinD. (**C**) The D_2E_2 complex. The open form of the MinE dimer (red) is stabilized upon interaction with the membrane-bound MinD dimer (cyan). The D_2E_2 complex is stably bound to the membrane via three MTSs, two from the MinD dimer and one from the MinE dimer. Structures for (B–C) were adapted from PDB ID 3R9J[11] and are used here for conceptual illustration purposes only. The highlighted MTSs of MinD and MinE were not present in the PDB structures.

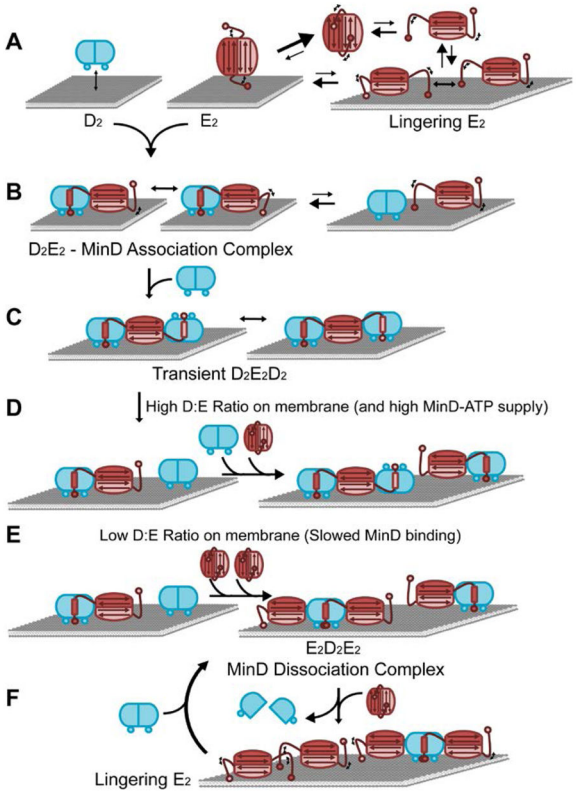

Fig. 3. MinD/MinE stoichiometry on the membrane drive patterning

(A) ATP-bound MinD dimers (D_2 - cyan) dynamically bind membrane. The closed form of the MinE dimer (E_2 – red) has a six-stranded β-sheet making its hydrophobic core. Conformational breathing of the MinE dimer allows for dynamic membrane binding via its MTSs (red circles). **(B)** D_2E_2 complex formation stabilizes membrane association for both proteins. One MinD binding site is still available on the MinE dimer for interaction with another MinD dimer. **(C)** This second MinD binding site recruits more MinD from solution and forms a transient $D_2E_2D_2$ complex. **(D)** During pattern initiation, all MinE dimers on the membrane are in complex as D_2E_2 or $D_2E_2D_2$. **(E)** As MinE accumulates on the membrane, $E_2D_2E_2$ complexes can form, which stimulate ATP hydrolysis and MinD release from the membrane as monomers. **(F)** MinE dimers lingering on the membrane after MinD release prevent MinD from rebinding the membrane.

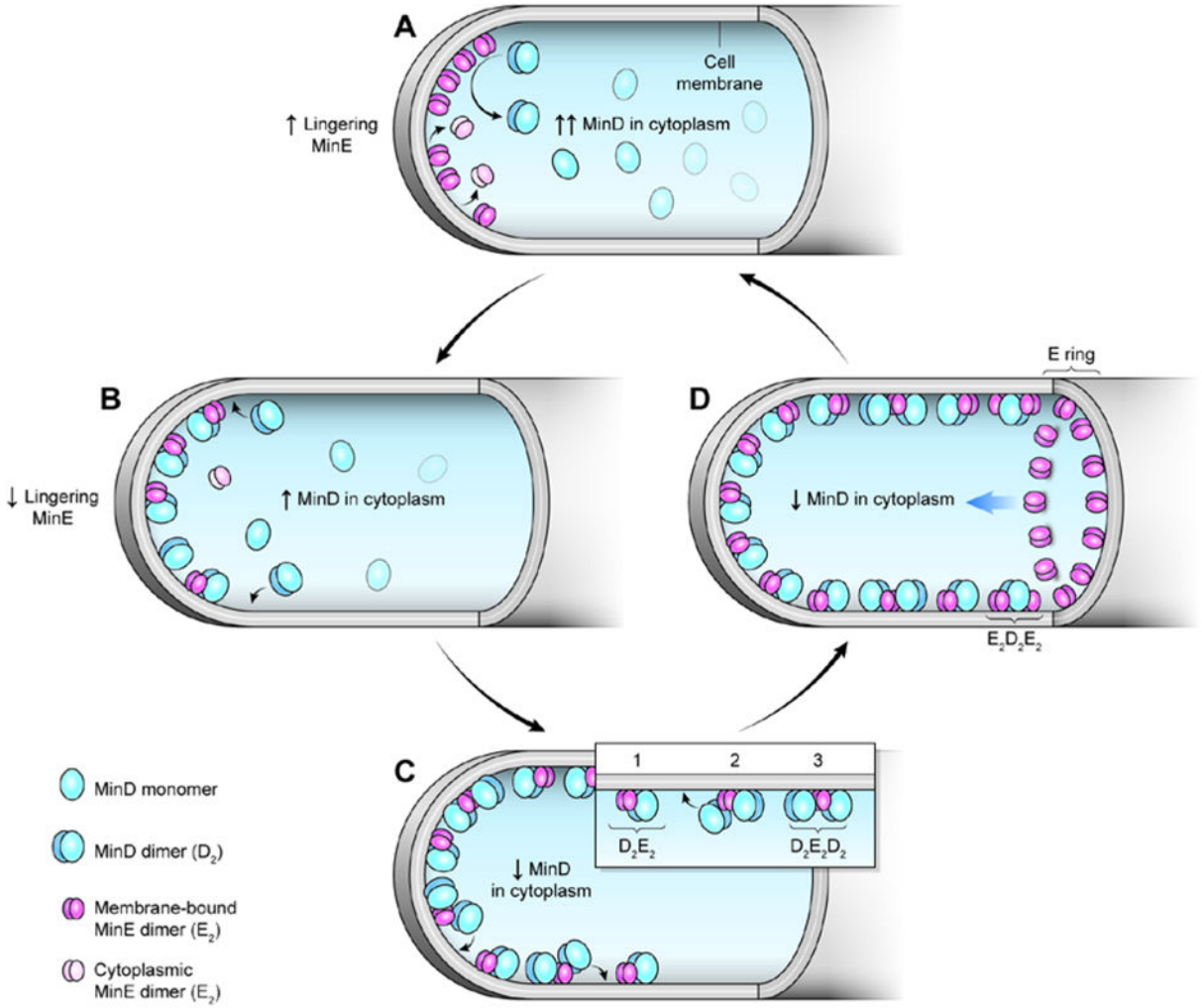

Fig. 4. Molecular model of Min oscillation *in vivo*

(**A**) At high density, lingering MinE provides the refractory period for immediate MinD rebinding at the cell-pole from which it just dissociated. (**B**) Once the lingering MinE density declines, MinD dimers can bind the membrane and join MinE dimers in a one-to-one complex. (**C**) This D_2E_2 complex then stimulates the recruitment of another MinD dimer, to form $D_2E_2D_2$. (**D**) As active MinD dimers deplete from the cytoplasm and MinE dimers accumulate on the membrane, $E_2D_2E_2$ can form, where a MinD dimer is now sandwiched by two MinE dimers. This complex stimulates MinD release while lingering MinE dimers concentrate into an E-ring that continues to disassemble MinD from the polar zone. The process then repeats.

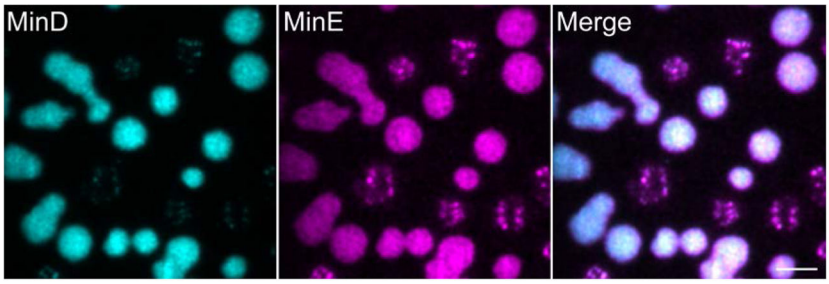

Fig. 5. Standing-wave bursts

Freeze frame image of MinD (cyan) and MinE (magenta) forming the burst pattern. Bursts formed as part of a pattern spectrum reconstituted as described in Figure 1. Bursts formed near the flowcell outlet where the protein supply is depleted. Scale bar = 10 μm. Adapted with permission from [2].

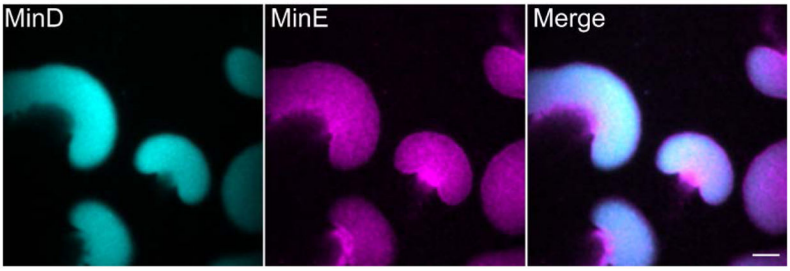

Fig. 6. Travelling Mushrooms

Freeze frame image of MinD (cyan) and MinE (magenta) forming the mushroom pattern. Mushrooms formed as part of a pattern spectrum reconstituted as described in Figure 1. Mushrooms formed near the midpoint of the flowcell where the protein supply is pseudo-depleted. Scale bar = 10 μm. Adapted with permission from [2].

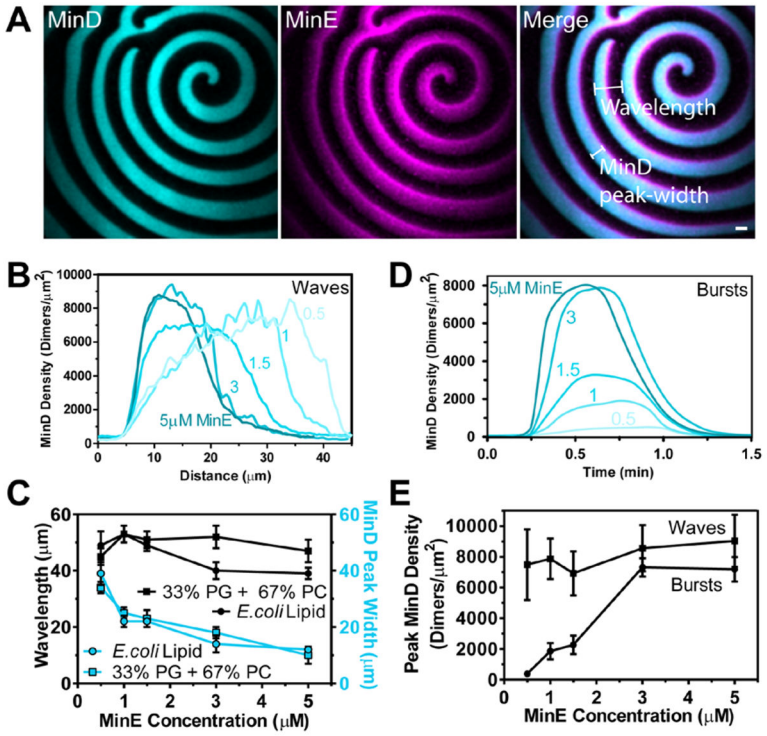

Fig. 7. Traveling waves versus standing-wave bursts

(**A**) Freeze frame image of waves supported by MinD (cyan) and MinE (magenta). The wavelength is the distance from one wave front to the next (see merge). MinD “peak-width” is the distance from the wave front to the MinE-rich rear where MinD has dissociated. Scale bar = 20 μm (**B**) The MinD peak-width narrows as the solution concentration of MinE increases. (**C**) Although MinD peak-width narrows with increasing MinE (cyan), the wavelength remains constant (black). (**D**) The rates of MinD accumulation and dissipation, as well as the peak MinD density in bursts increase with increasing MinE concentration. As a result, the temporal periodicity did not change. (**E**) Regardless of MinE concentration, waves have a saturating protein density on the SLB, which is responsible for the transition to protein release at the rear of a wave. Bursts on the other hand start the dissipation phase due to solution depletion of active MinD dimers. Data reproduced and combined from Vecchiarelli *et al.*, 2014 and Vecchiarelli *et al.*, 2016.

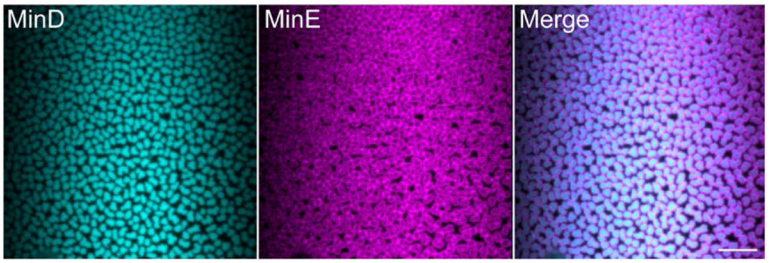

Fig. 8. Amoebas

Freeze frame image of MinD (cyan) and MinE (magenta) forming the amoeba pattern. Amoebas formed as part of a pattern spectrum reconstituted as described in Figure 1. Amoebas formed near the inlet of the flowcell where the protein supply is very high. Scale bar = 10 μm. Adapted with permission from [2].